A Customer Centric Approach to the Use of Residential Batteries for Distribution Network Support

S. R. Deeba, *Member, IEEE,* P. Barooah, *Senior Member, IEEE,* R. Sharma, *Senior Member, IEEE,* J. Brooks and T. K. Saha, *Senior Member, IEEE*

***Abstract*—This paper proposes and practically validates – a control approach for distribution network (DN) support with customers' battery energy storage systems (BESSs). Use of customers' BESSs for DN support lead to a cost (disutility) to customers, since a part of the storage capacity is used for DN support instead of solely benefitting the customer. An optimization problem is formulated to perform a trade-off between the benefits to network operator and disutility to consumers. Control actions, i.e., charge and discharge trajectories of BESSs, are obtained by solving the optimization problem. Hardware in the loop (HIL) simulations of the proposed method, using a real-time digital simulator and a dSPACE controller board, are performed to assess its performance on a low voltage distribution network. HIL simulations show that in the presence of rooftop solar, the method is able to reduce voltage excursions while simultaneously reducing customers' cost.**

***Index Terms*—Battery storage, battery control, demand response, voltage regulation.**

NOMENCLATURE

Sets

N	Set of total bus indices
L	Set of load bus indices
H	Set of infinite bus indices

Parameters

n	Total number of nodes
p	Number of loads
m	Number of BESS connected nodes
$Y_{n\times n}$	Bus admittance matrix
θ	Bus admittance angles
η	BESS efficiency
α	Voltage penalty factor
β	Real power flow penalty factor
γ	Reactive power penalty factor of BESS
a_1	Disutility convex co-efficient
V_{min}	Minimum voltage magnitude per unit
V_{max}	Maximum voltage magnitude per unit
TVR	Possible duration for voltage regulation

Exogenous variables (per unit)

P_l	Real power demand
Q_l	Reactive power demand
P_{PV}	Real power from solar PV
Q_{PV}	Reactive power from solar PV
P_{gmin}	Minimum real power drawn from grid
P_{gmax}	Maximum real power drawn from grid
E_{imax}	Maximum kWh capacity of BESS
P_{Bmin}	Minimum real power of BESS
P_{Bmax}	Maximum real power of BESS
Q_{Bmin}	Minimum reactive power of BESS
Q_{Bmax}	Maximum reactive power of BESS
S_{max}	Maximum VAR capacity of a BESS inverter
P_{BTH}	Threshold real power of BESS
SoC	Current State of charge of BESS
SoC_{min}	Minimum state-of-charge of BESS
SoC_{max}	Maximum state-of-charge of BESS

State and control variables (per unit)

P_g	Real power drawn from grid
Q_g	Reactive power drawn from grid
V	Bus voltage
δ	Bus voltage angle
P_B	Real power of BESS
Q_B	Reactive power of BESS

S. R. Deeba, R. Sharma and T. K. Saha are with the School of ITEE, The University of Queensland, Australia. (e-mail corresponding author: rahul.sharma@uq.edu.au)

P. Barooah and J. Brooks are with the University of Florida, USA; their work is partially supported by the National Science Foundation through grant 1646229 and by the Dept. of Energy through a Grid Modernization Laboratory Consortium.

I. INTRODUCTION

Renewable energy generators such as solar photovoltaic (PV) systems mitigate greenhouse gas emissions associated with electricity generation. Through favorable policies and incentives, there has been a remarkably rapid growth in PV installations in low voltage distribution networks. The bidirectional flow of active power in distribution networks (DNs) caused by residential PV generation causes undesirable voltage rise. Low voltage (LV) distribution networks are particularly susceptible to voltage excursions due to high resistance to reactance (R/X) ratios [1]. High PV situations in LV networks substantially increase the likelihood of violation of the voltage limits specified by IEEE-1547 [2].

There has been a lot of research on voltage regulation in LV distribution networks (see e.g. [3],[4] and references therein). For voltage management, distribution network operators (DNO) currently rely almost entirely on the use of equipment such as on-load tap changing transformer (OLTC) at substations, step-voltage regulators (SVR) and fixed capacitors. However, the existing OLTCs and SVRs are not designed for voltage regulation under reverse power flow, which can cause excessive use of tap-changers resulting in accelerated wear/tear of equipment [5]. Another approach to support network voltage is through the use of residential inverters (e.g. [6], [7]). To implement this approach, grid codes and standards have been updated (for example IEEE 1547) to allow reactive power support through residential inverters. The main limitation of such an approach is that larger inverters may be required to deliver a specific amount of real power (governed by the PV panel rating) at a non-unity power factor.

Meanwhile, the rise in PV penetration is accompanied by the rise in Battery Energy Storage Systems (BESSs) uptake at residential levels. The BESSs are also a novel resource that are useful for providing network support. Therefore, the use of BESSs for distribution network support has been a subject of active research in recent years. A diverse set of approaches have been proposed with varying goals, e..g, for voltage and/or frequency regulation [8], [9], [10], minimization of line losses, equipment degradation cost, operational cost, or a combination thereof [11], [12], [13], [14]. The focus has been on maximizing benefits to DNOs without much thought about the cost to consumers.

Use of a BESS for anything other than the use intended by the customer potentially causes a loss to the customer. BESSs provide customers an ability to arbitrage: the customer can use locally generated solar energy stored in the BESS during peak demand periods when grid-supplied electricity is more expensive. In many areas of the world, customers' can also use their BESS to participate in demand response (DR) programs and generate revenue. If customers' BESS capacity is partially used for network support, it is likely to come at the expense of their planned arbitrage or DR use, resulting in an opportunity cost. The trade-off between benefit to DNOs and loss to customers has not been adequately addressed in the literature. In this paper, we present an approach for controlling customers' BESS to provide distribution network support in LV distribution networks that strikes a balance between benefit to DNOs and cost to customers. Apart from the economic cost to consumers described above, there may also be a non-economic cost stemming from the perceived loss of control of their own resource. Therefore we model the consumer cost as a *disutility*, which is a function of the deviation from a nominal operation [15], [16]. The nominal operation is the one that is most economically beneficial to the consumer, without considering any distribution network support function. Customers' disutility and the cost of violations in voltage regulation and peak power limits are utilized to formulate an optimization problem. Decisions for the BESSs charge/discharge trajectories are computed by solving this optimization problem.

The proposed method is then validated on a high-fidelity real-time HIL simulation setup comprising of an interconnection of Real Time Digital Simulator (RTDS) and a dSPACE controller board [17]. A radial LV distribution system is modeled in RTDS and the proposed controller is executed in dSPACE. Performance of the proposed method is evaluated under multiple simulation scenarios and is compared with conventional voltage regulation methods. The HIL simulations show that the proposed control scheme can reduce voltage rise compared to the baseline scenario in which BESS are not used for voltage support.

Many recent papers have focused on decentralized methods for coordination among BESS. Our focus is smaller LV networks, in which centralized control of the relatively smaller number of participating BESSs is considered adequate. We therefore limit ourselves to a centralized control architecture in this paper. This paper assumes that the proposed voltage control algorithm can be used either directly by the DNO or indirectly through a demand response aggregator (DRA) responsible for network support services. Figure 1 presents a typical configuration of aggregating customers' BESS in a radial distribution network. For the proposed control algorithm to be implemented, the BESS units are assumed to communicate with a central system, while the relevant data are accessed through smart meters.

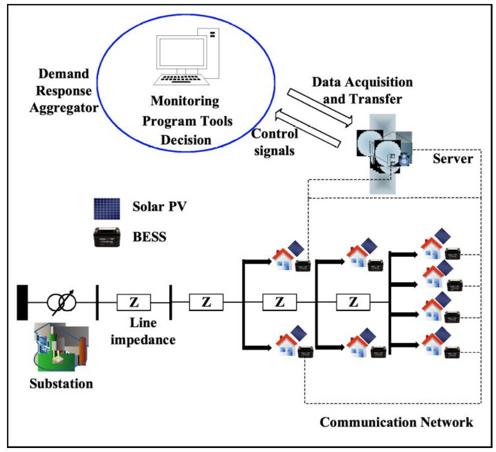

Figure 1: A typical control architecture for aggregating distributed resources

II. Proposed Control Algorithm

This section presents the mathematical model of a distribution network comprising of PV and BESS. The distribution network model is used in the formulation of an optimization problem that formulates the trade-off between reduction in financial benefits (disutility) to consumers and network voltage support benefits to DNOs.

A. Power Flow Model

A radial distribution network with n number of buses is considered and presented by the set $N := [N_1, N_2, N_3, \dots, N_n]$. Let L be the set of load buses in the network, where $L := [L_1, L_2, L_3, \dots, L_p]$. The set of BESS connected nodes is represented by B, where $B := [B_1, B_2, B_3, \dots, B_m]$. The network admittance is represented by the matrix $Y_{n \times n}$. Let H be the set of the buses through which the network is connected to the grid such that $H \subseteq N$.

If a particular node does not have a load that consumes real or reactive power or does not have a PV or BESS, the corresponding variables are set to zero. The active power (P_{Bi}) and reactive power (Q_{Bi}) of BESS are considered as the control variables, where $i \in [1, \dots, n]$. The state variables include real (P_{gi}) and reactive power (Q_{gi}) of the infinite bus. Voltage magnitudes (V_i) and angles (δ_i) of all the nodes are also considered as state variables. The state variables are presented by a set $Z_i := [P_{gi}, Q_{gi}, V_i, \delta_i]$, while the voltage magnitude and angle of the slack bus are known and not included in the state vector. The real and reactive power flow problems at i^{th} node of a balanced three phase system can be expressed by (1)-(2) [18]:

$$P_{gi} + P_{PVi} + P_{Bi} - P_{li} = \sum_{j=1}^{n} |V_i|\,|V_j|\,|Y_{ij}| \cos(\theta_{ij} + \delta_j - \delta_i) \quad (1)$$

$$Q_{gi} + Q_{PVi} + Q_{Bi} - Q_{li} = -\sum_{j=1}^{n} |V_i|\,|V_j|\,|Y_{ij}| \sin(\theta_{ij} + \delta_j - \delta_i) \quad (2)$$

While most practical networks are unbalanced, the consideration of a balanced network model is acceptable because most of the end use (residential) customers (e.g. in Australia) are connected to single phases. The use of balanced approach is accompanied with computational benefits that are necessary for the practical online implementation of the proposed controller. Any controller that relies on nonlinear programming is likely to exhibit computational challenges, thereby any optimality benefits will render unrealisable in practice. Successful validation of a approach developed using a balanced model on a single phase of an unbalanced network confirms the robustness of the proposed approach to any modelling errors.

B. Disutility to Customers

The customer centricity of the proposed approach is underpinned by the use of a 'disutility function' that models the potential negative effect of leveraging customer BESS for network support. Customers are often given incentives (e.g. Feed-in-Tariff and Time of Use) for PV power export. However, many utilities around the world are gradually closing or significantly reducing the feed-in-tariff incentives. In the absence of any such incentives, customers are not financially benefitted for power export. This paper assumes that financial incentives are absent. Without any incentives on solar PV, the most economic option is to store the excess PV energy in a BESS during the day and utilize the stored energy when solar power is not available. To this end, a financially optimum choice of charging/discharging rate of the i^{th} BESS at any instant (being denoted as P_{BTHi}) can be expressed as

$$P_{BTHi} = P_{li} - P_{PVi}\,;\ \forall\, i \in [1, n] \quad (3)$$

where, P_{li} and P_{PVi} indicate the customer's load and PV power respectively at i^{th} node and displayed in Figure 2. If the $P_{li} > P_{PVi}$, the sign of P_{BTHi} is positive which indicates discharging of BESS. The negative sign of P_{BTHi} indicates charging of BESS when $P_{li} < P_{PVi}$.

It is understood that variations in the BESS charge/discharge rates from P_{BTHi}, in order to provide network voltage support, will impose a cost to customer. A BESS charge rate higher than P_{BTHi} implies higher charging from the grid than the most economic, while a charge rate less than P_{BTHi} means exporting PV power to the grid when it is not most economic to do so. Higher discharging of a BESS also reduces its lifetime. Any additional incentives paid to consumers (BESS owners) are assumed to be in the form of a flat rate and, therefore, are not considered. To model these costs, the following disutility function is introduced:

$$f(P_{Bi}) = a_1 (P_{Bi} - P_{BTHi})^2\,;\ \forall\, i \in [1, n] \quad (4)$$

where $a_1 \geq 0$ is a modeling parameter whose value depends on the cost of using BESS (in \$/kW) for network voltage support. The quadratic nature of the disutility is inspired by the fact that variable cost of electricity generators is usually modeled as a quadratic function of generated power [19], and also by the quadratic model of consumer disutility used in [15], [16]. Figure 2 illustrates the disutility function.

The role of f is to impose a cost on deviation from the consumer's planned arbitrage in order to provide voltage regulation with their BESS. The subsequent optimization discussed next is aimed at computing a charge-discharge rate of BESS. It provides voltage regulation that is a benefit to the DNO, while balancing the cost to a DR aggregator as modeled by the disutility function.

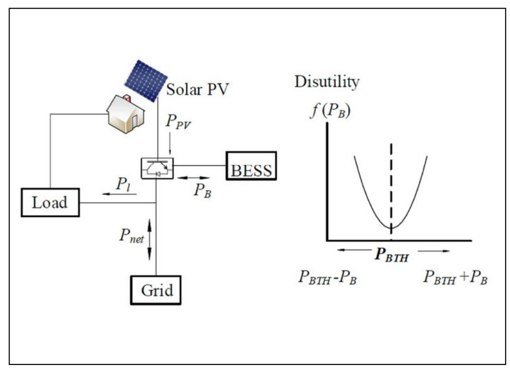

Figure 2: Threshold BESS output and customer's disutility modeling

C. Optimization Problem Formulation

The input data for the problem are P_{PVi}, Q_{PVi}, P_{li}, Q_{li}, V_j and δ_j, where $i \in [1, \ldots, n]$ and $j \in H$. It is assumed that the smart meters are configured to measure the above data. Given a specific choice of the control variables P_{Bi} and Q_{Bi}, there are $(n \times 2)$ unknowns, which can be determined from the $(n \times 2)$ power flow equations, assuming a solution exists.

1) Objective function: Let J be a function that models the cost to the relevant stakeholders (consumer and DNO). The cost function is defined as follows:

$$J(P_{Bi}, P_{gi}, Q_{Bi}, V_i) = \sum_{i=1} f(P_{Bi}) + \alpha |V_i - 1|^2 + \beta P_{gi}^2 + \gamma Q_{Bi}^2 \quad (5)$$

where $\alpha \geq 0$, $\beta \geq 0$ and $\gamma \geq 0$ are the tuning parameters. The first term of the cost function is consumer's disutility as explained in subsection II-B. The second term helps in keeping the bus voltage close to unity by choosing a large value of the voltage penalty factor α. The third term helps in peak shaving. Keeping the bus voltages near unity is in the interest of voltage regulation and is consistent with peak shaving. The fourth term of the cost function is to penalise reactive power injection from the BESS since there are restrictions on power factors of inverters in many power systems.

The minimization of (5) has to be done while respecting various constraints. These constraints are described next.

- *Limits on Total Power Flow in a Network*: The following constraints are formulated to control the total real and reactive power flow:

$$P_{gi\,\min} \le P_{gi} \le P_{gi\,\max} \;\; ; \forall\, i \in [1, n] \tag{6}$$

$$Q_{gi\,\min} \le Q_{gi} \le Q_{gi\,\max} \;\; ; \forall\, i \in [1, n] \tag{7}$$

  This constraints impose limits on the power import from the grid that may be desirable for stakeholders (such are retailers, DNOs and consumers). Maintaining peak power drawn from the grid within acceptable limits reduces the chance of transformer overloading, therefore, is consistent with the interests of a DNO.

- *BESS Capacity Constraints*: The required amount of energy (E_{avi} kWh) for full charging of a BESS from the present state at i^{th} node is expressed by (8).

$$E_{avi} = (1 - SoC_i)E_{i\,\max} \quad \forall\, i \in [1, n], \tag{8}$$

  where SoC_i is the state of charge of the i-th node, and E_{imax} (kWh) is the maximum BESS capacity at i^{th} node. Then, the maximum limits of real and reactive power of BESS at an instant are expressed by (9)-(10).

$$P_{Bi\,\max} = \frac{E_{avi}}{T_{VR}} \;\; ; \forall\, i \in [1, n] \tag{9}$$

$$Q_{Bi\,\max} = P_{Bi\,\max} \,.\, \tan\{\cos^{-1}(p.f.)\}, \forall i \in [1, n] \tag{10}$$

  where T_{VR} indicates the possible duration for voltage regulation and is given as an input to the optimization problem. Reactive power limit at an instant is calculated based on the power factor (p.f.) standards for small scale BESS inverters defined by IEEE 1547. The two limits expressed in (9) and (10) are utilized to formulate the following constraints.

$$P_{Bi\,\min} \le P_{Bi} \le P_{Bi\,\max} \;\; ; \forall\, i \in [1, n] \tag{11}$$

$$Q_{Bi\,\min} \le Q_{Bi} \le Q_{Bi\,\max} \;\; ; \forall\, i \in [1, n] \tag{12}$$

  The value of P_{Bimin} and Q_{Bimin} can be 0 or equal to $-P_{Bimax}$ and $-Q_{Bimax}$ respectively. It may be noted that, in the absence of PV, the BESS operation is limited by the lower limit of SoC. The sizes of BESS units are assumed to be sufficiently large to store the surplus energy generated by PV. This assumption implies that the perturbations around the financially optimum BESS profile will not result in SoC constraint violation. Nevertheless, SoC constraints can also be easily included in this formulation.

- *Node Voltage Constraints*: The voltage of the BESS connected nodes is controlled within standard limits and expressed by (13).

$$V_{\min} \le V_i \le V_{\max} \;\; ; \;\forall\, i \in [1, m] \tag{13}$$

- *BESS Inverter Size*: The real and reactive power of BESS must be selected in such a way that can reside under the inverter's maximum capacity limit as expressed by (14).

$$(P_{PVi} + P_{Bi})^2 + Q_{Bi}^2 \le S_{i\max}^2 \;\; ; \forall\, i \in [1, m] \tag{14}$$

  where, S_{imax} implies the maximum volt-ampere capacity of the BESS inverter. The goal is to pick P_{Bi} and Q_{Bi} that minimises J and for which the corresponding P_{gi}, Q_{gi}, V_i, δ_i (obtained from power flow equations) satisfy the relevant inequality constraints given by (1)-(2), (6)-(7) and (11)-(14).

The decision vector is $x := [P_{Bi}, Q_{Bi}, P_{gi}, Q_{gi}, V_i, \delta_i]$. The load-flow equations (1) and (2) are expressed in the form of $g(x) = 0$. An inequality in the form of $a \le x \le b$ is equivalent to $x-b \le 0$ and $-x+a \le 0$. Therefore, all the inequality constraints in (6)-(7) and (11)-(14) are compactly represented as $h(x) \le 0$. The expression of the inequality constraints is given by (15).

$$h(x) = \begin{bmatrix} A_h \,.\, x - b_h \\ C_h \,.\, x^2 - S_{\max}^2 \end{bmatrix} \tag{15}$$

The expressions of A_h, b_h and C_h for a two nodes system with a single BESS are as follows:

$$A_h = \begin{bmatrix} 1 & 0 & 0 & 0 & 0 & 0 \\ -1 & 0 & 0 & 0 & 0 & 0 \\ 0 & 1 & 0 & 0 & 0 & 0 \\ 0 & -1 & 0 & 0 & 0 & 0 \\ 0 & 0 & 1 & 0 & 0 & 0 \\ 0 & 0 & -1 & 0 & 0 & 0 \\ 0 & 0 & 0 & 1 & 0 & 0 \\ 0 & 0 & 0 & -1 & 0 & 0 \\ 0 & 0 & 0 & 0 & 1 & 0 \\ 0 & 0 & 0 & 0 & -1 & 0 \end{bmatrix};$$

$$b_h = \begin{bmatrix} P_{B\,\max} \\ -P_{B\,\min} \\ Q_{B\,\max} \\ -Q_{B\,\min} \\ P_{g\,\max} \\ -P_{g\,\min} \\ Q_{g\,\max} \\ -Q_{g\,\min} \\ V_{\max} \\ -V_{\min} \end{bmatrix}; \quad C_h = \begin{bmatrix} 1 \\ 1 \\ 0 \\ 0 \\ 0 \\ 0 \end{bmatrix}.$$

Once the constraints are rewritten as $g(x) = 0$ and $h(x) \le 0$, the goal is to pick x that solves the following optimization problem expressed by (16) and (17).

$$\min_x \; J(x) \tag{16}$$

subject to:

$$g(x) = 0, \quad h(x) \le 0 \tag{17}$$

The cost and inequality constraints are convex functions of x, while the equality constraints are non-linear and non-convex [18]. Therefore, a suitable solution method is required to solve the problem for optimum solutions at every sampling instant.

D. Solution Method

The problem as described in Subsection II-A is non-convex due to the non-linear equality constraints originating from power flow equations. A convex relaxation of this problem is obtained by approximating this nonlinearity by a linear equality by Jacobian linearisation around an operating point. For Jacobian linearisation, let x_0 be a nominal operating point. Let $\Delta x = x - x_0$ so that the equality constraint can be linearised to $g(x_0) + \nabla g(x_0)\Delta x = 0$, which is expressed by:

$$A_h \,\Delta x = b_h \tag{18}$$

where $A_h = \nabla g(x_0)$ and $b_h = -g(x_0)$. Now, the problem can be defined by (19) and (20).

$$\tilde{J}(\Delta x) := J(x_0 + \Delta x) \tag{19}$$

$$\tilde{h}(\Delta x) := h(x_0 + \Delta x) \tag{20}$$

Based on the aforementioned definitions, the formulated problem can be updated to the following form:

$$\min_{\Delta x} \tilde{J}(\Delta x) \tag{21}$$

subject to the constraints as expressed by (22) and (23):

$$A_h \Delta x = b_h \tag{22}$$

$$\tilde{h}(\Delta x) \leq 0 \tag{23}$$

The convexity of J and h ensures that the respective $\tilde{J}$ and $\tilde{h}$ are convex, which makes (21)-(23) a convex problem. The log-barrier interior point method is used to search for the optimum point of the above problem [20]. The searching starts with a point x_0 such that it satisfies $g(x_0) = 0$, which is accomplished through root finding. The resulting solution is checked to ensure no violation of the original, non-approximated, constraints. If any constraint is violated, the relaxed problem is iteratively solved by adjusting the real and reactive power of BESS to find a feasible point.

III. System Description and Modeling

In this work, IEEE-13 nodes system, shown in Figure 4 is used to test the BESS controller. At present, there are no standard test models to represent residential customers in a network. In fact, the regulations in some countries (such as Australia) prohibit use of residential customer data by network utilities. While the regulations are likely to undergo amendments in the near future, for the sake of the validation of the proposed approach a 13-bus system is considered as a representation of a practical system and the control validation can be seen as an implementation on aggregate customer BESS resources and loads. Nevertheless, the same concepts apply for a network specific to residential customers. Although an unbalanced network is considered for the validation of the proposed approach, the actual implementation of the proposed control is on nodes 611 and 684 that are connected to phase C of node 671. Consequently, the implementation of the proposed control is on a single phase end of an overall unbalanced network. Hence, the control design and its implementation are consistent. The 13-bus unbalanced system is chosen a representative of a realistic network configuration. Any effects due to magnetic coupling (e.g. if the phases are on the same 'power corridor') or model mismatch that can somewhat compromise the validity of the optimal solution can be taken into account through the provision of tightening of the constraints so that model mismatch induced sacrifice of optimality does not result in violation of constraints in practical systems.

Hardware-in-the-loop validation is performed using RTDS and dSPACE. RTDS is an industry standard for performing high-fidelity power system simulations. dSPACE is a standard rapid control prototyping system which is widely used for validation and testing of control algorithms. Collectively, validation on the RTDS-dSPACE setup provides a high level of confidence in the validity of the proposed approach which is desirable in comparison to a desktop-based simulation validation. This section describes the studied network and the simulation setup.

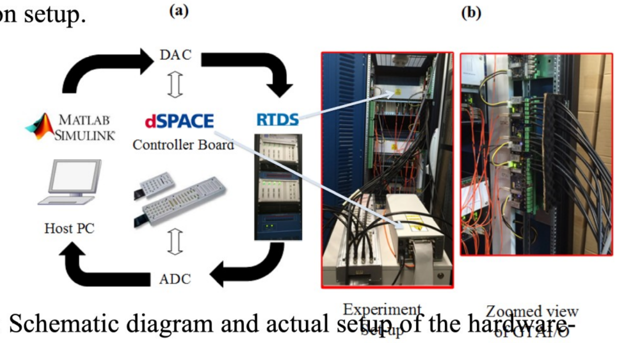

Figure 3: Schematic diagram and actual setup of the hardware-in-the-loop set-up

A. Simulation HIL Setup

The HIL setup involves RTDS, dSPACE and a host PC. A schematic of the high-fidelity real-time simulation setup of the RTDS-dSPACE is presented in Figure 3. RTDS package comprises of both hardware and software parts. The software platform RSCAD is utilized to model components of the network such as unbalanced impedance, single and three phase loads, transformer, solar PV and BESS. The analog input/output ports of Gigabit Transceiver Cards (GTI/O) are used to access analog signals from RTDS.

The dSPACE is an external rapid control prototyping system, which comprises several ADC and DAC channels. The dSPACE has a processor unit (DS1103), which is interfaced with a host computer through a PCI card and a TX/RX optical link. The proposed BESS control approach is implemented in MATLAB/Simulink and the respective C-code is downloaded on dSPACE. While running the power flow of RTDS network, it results in all node voltage magnitudes, angles and real-reactive power flow through lines. The analog data from the RTDS power flow simulation is accessed via a GTAO card and entered to the dSPACE control device through RG6 cables. The analog signals of the RTDS network is processed to digital using ADC channels of dSPACE and then is utilized in the proposed control algorithm to generate control signals for a BESS. The controller outputs from dSPACE are then passed on to the BESS model in RTDS via DAC channels. The sampling period of the Simulink program is selected in such a way that the control algorithm can execute within the sampling interval. The distribution network runs in RTDS at a 50 μs sampling rate, while the Simulink program is executed in a few seconds.

B. IEEE-13 Nodes Feeder with PV and BESS

The studied IEEE-13 nodes system contains several spot and distributed loads, which are modeled as constant impedance, current and power (ZIP) [21]. The voltage level of the network is 4.16 kV while it is connected to a 115 kV infinite bus through a 5000 kVA substation at the node 650. The network has single, two and three phase lines with unbalanced characteristics. It has seven line configurations with different R/X ratios, which makes it a close resemblance to practical systems. There are two voltage-regulating devices: OLTC transformer in the substation and fixed capacitors at the nodes 611 and 675. The OLTC model used in the simulations is taken from the RTDS library and is consistent with standard industry practice. The model utilizes an autotransformer and a control

Table I: Parameter values used in the case studies

Parameters	Value
SoC_{min}	10%
SoC_{max}	90%
V_{min}	0.94 p.u.
V_{max}	1.055 p.u.
P_{gmin}	-5 p.u.
P_{gmax}	5 p.u.
S_{imax}	1 p.u.

circuit to implement a three phase regulating transformer rated 5000 kVA, 115/4.16 kV and delta-wye configuration to regulate voltage at 4.16 kV bus of the studied system. A large-scale solar PV of 100 kW rating is placed at the node 611 to simulate the voltage rise phenomenon. A sufficiently high R/X ratio (> 10) is assumed for the connecting single phase line between the nodes 684 and 611. A BESS is placed at the same locations of PV to regulate the point of common coupling (PCC) and upstream node voltages. Figure 4 presents the schematic diagram of the IEEE-13 nodes distribution system with PV and BESS. A detailed model of BESS is used for RTDS simulation, which includes a battery bank, voltage source inverter and inverter controller [22]. Inverter

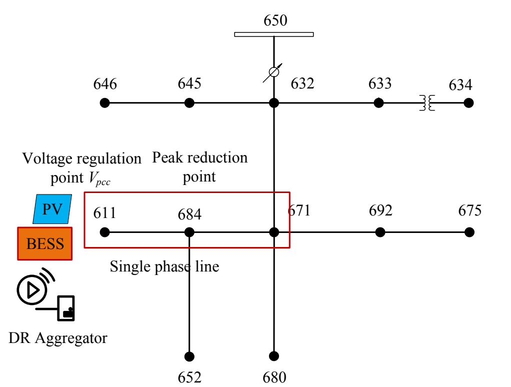

Figure 4: A Schematic diagram of the modified IEEE-13 nodes feeder [20]

controller is implemented using the standard RTDS block-set and comprises of a phase locked loop (PLL) and a current regulator [22].

IV. Results and Discussion

The performance of the developed control algorithm is evaluated through several simulation scenarios. In the beginning, a base-case load flow of the IEEE-13 node system is simulated, without a BESS but otherwise identical to the system described in Figure 4. Then, several case studies are performed with the BESS. The performance of BESS controller is scrutinised under different parameter values. The nominal values of the parameters of the proposed controller are presented in Table I. All the values related to voltage and power are provided in p.u. considering the base power of the system as 1000 kVA.

A. Base Case (Voltage Regulation with OLTC and without BESS)

A variable PV power profile for 7.5 hours is considered, while loads remain consistent at 118 kW. The PV power rises to 120 kW in the mid-noon, which causes a very light

Table II: Parameter values used in the case studies

Parameters	Value ($\times 10^{-6}$ \$)
a_1	1000000
α	10000
β	10
γ	10000

net load at PCC. Figure 5(a) shows the PV power and the customer's load profiles. The fluctuating PV output causes voltage fluctuation at nodes 611 and 684 as shown in the Figure 5(b). It can be observed from Figure 5(b) that PCC voltage reaches above the upper limit (1.065 p.u) in the noon-time due to high PV generation. Therefore, a window of the PV power profile from the time 8:30 to 17:30 is chosen to test the proposed BESS controller in the subsequent case studies.

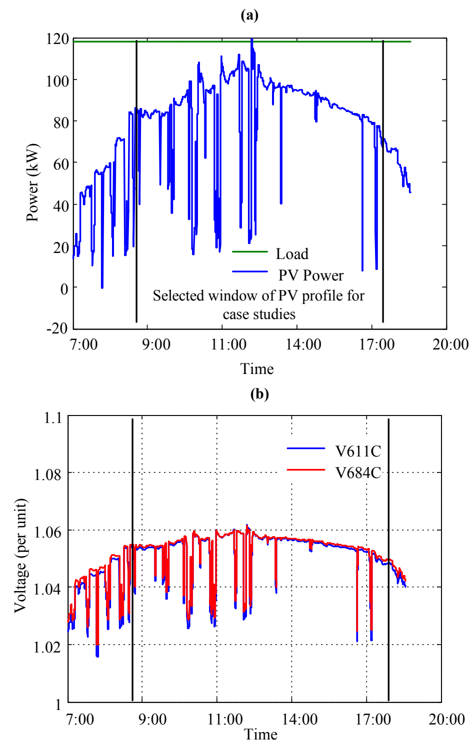

Figure 5: (a) Solar PV output and load at the PCC (b) PCC voltage profile

B. Voltage Performance with BESS (with $\alpha > 0$)

Table II shows the values of the parameters a_1, α, β and γ in this case, while these values are chosen arbitrarily and are varied. The values of the parameters are scaled by 10^{-6} for conversion of the total cost associated with voltage regulation in \$ at each sampling instant. The disutility convex coefficient a_1 is selected sufficiently large to match per unit conversion of the respective variables. Higher values of disutility coefficient imply costlier BESS operation for customers, which imposes more cost to the aggregators. The voltage penalty factor is chosen a large value to restrict voltage deviation from unity. The weight on β has been kept low to relax the peak power flow of the network while the weight on reactive power penalty γ is chosen reasonably large so that it does not end up using much reactive power of BESS. The real and reactive powers of the BESS and respective PV and load profiles are presented in Figure 6(a). It is observed that the BESS

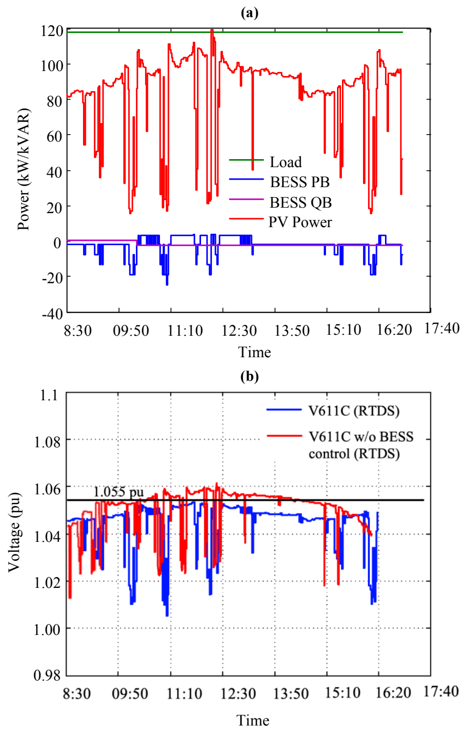

Figure 6: Voltage performance of the studied feeder with a positive value of α (a) PV, load and BESS power at PCC (b) Voltage profiles of the studied nodes

is charged at a variable rate from 8:30 until 10:00 hrs and then it starts discharging for a while. The charge-discharge continues for the rest of the day. As presented in Figure 6(b), the voltage magnitudes of nodes 611 and 684 is well maintained within 0.94 to 1.055 p.u. limits. It can be seen from Figures 6(a) and (b) that if PV output rapidly rises and results in a higher voltage ($>$ 1.055 p.u.) at the studied nodes, the BESS is discharged at such a rate that it regulates the voltage closer to the upper limit (1.055 p.u.). This is due to the high value of parameter a1, which imposes a higher cost for increasing BESS charge rate. Therefore, instead of charging at a high rate, the proposed control algorithm decides to discharge BESS at a low rate keeping the voltage within specified limits. It is also observed from Figure 6(b) that the predicted voltage at node 611 by the proposed method in dSPACE mostly matches the actual node voltage in RTDS with a negligible error ($<$ 1%). Therefore, it is evident that the proposed formulation is capable enough to present the accurate system behaviour with BESS. In the HIL simulation, the proposed approach in dSPACE receives the feasible initial values of the respective state variables from RTDS at every sampling instant.

C. Comparing the operating regions for different voltage penalty

Figure 7 is generated by using equations (4) and (5). The red curves are generated using equation (4) with a range $\alpha \geq 0$ values. The dashed green curve represents $\alpha = 0$, therefore, represents cost function without any penalty on voltage straying away from 1 p.u. It is clear from Figure 7 that by choosing an appropriate $\alpha > 0$ value, the minimum achievable cost of voltage regulation using BESS can be lowered. Without the voltage penalty term in (5), the voltage regulation is solely due to the constraint on voltage (13).

The controller performance is further checked for different values of tuning parameters a_1, α, β and γ. In this particular simulation setup, the ranges of parameters for which optimization problem remains feasible are found to be $a_1 \in [0, 1]$, $\alpha \in [0, 0.001]$, $\beta \in [0, 0.00001]$ and $\gamma \in [0, 0.2]$, however, the actual value and range of each parameter is governed by practical considerations and have to be established on a case by case basis. Nevertheless, some generic guidelines can be followed in tuning the parameters.

- The disutility convex coefficient a_1 governs the penalty on the usage of BESS for network support and, in particular, increasing a_1 discourages the use of BESS for network support. α, β and γ govern the voltage regulation, peak shaving and reactive power support.
- Increasing the value of α forces the algorithm to yield voltage close of 1 p.u. However, the permissible value of α is upper bounded by factors including available PV generation, load and available BESS capacity that govern the feasibility of the optimization problem.
- Increasing the values of β and γ discourages the power drawn from the grid (PG) and the reactive power support provided by BESS (QB), respectively. For example, setting γ large (e.g. γ = 0.002) results in no reactive power support from BESS (i.e. $Q_B = 0$), while setting $\gamma = 0$ results in $Q_B = -0.05$ p.u.

The effect of the choice of parameters is illustrated through three simulation scenarios whose results are presented in Table III. It is observed that at set point-1, the optimizer chooses BESS charging at 20 kW rate at a unity power factor. At set point-2, with the same values of a_1, α and β, if no restriction is imposed on the BESS reactive power (i.e. setting $\gamma = 0$), BESS is charged at a lagging power factor. For set point-3, the parameters a_1, α and γ are reduced. In this case, the BESS discharges with a lagging power factor. Since the objective function (5) comprises of multiple conflicting objectives, feasibility of the optimization problem guarantees that the values acquired by the variables will fall within the specified constraints but that does not automatically guarantee that the solution of the optimization problem will be consistent with the solutions expected for a single-objective optimization (e.g. voltage regulation only). The purpose of Table III is to demonstrate the impact of controller parameters on BESS performance and the corresponding values that the variables acquire. Between set-points 2 and 3, although choice of γ is changed from 0 to 200, simultaneously, the values of a_1 and β between the two set-points are chosen with significantly different values. Consequently, the resulting Q_B value remains the same for set-point-2 and set point-3. The impact of γ on the values of Q_B is visible from Set-point-1 whereby a large γ results in $Q_B = 0$

The disutility co-efficient a_1 is designed to be determined by a DRA based on the customers' actual disutility for BESS utilization in voltage regulation. From the value of disutility function, the DRA decides the payable amount to a customer. The total cost of a DRA for voltage regulation can be utilized

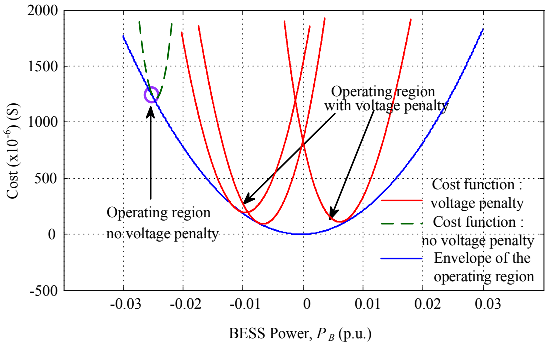

Figure 7: Operating regions of BESS with and without voltage penalty

Table III: Impact of controller parameters on BESS operation

Set point-1 (P_l = 118 kW, P_{PV} = 100 kW)				
Parameters	a_1	α	β	γ
Values (×10^{-6})	1000000	1000	10	20000
Variables	P_B	Q_B	V_{611}	δ_{611}
Results (p.u.)	-0.02	0	1.041	3.13
Set point-2 (P_l = 118 kW, P_{PV} = 100 kW)				
Parameters	a_1	α	β	γ
Values (×10^{-6})	1000000	1000	10	0
Variables	P_B	Q_B	V_{611}	δ_{611}
Results (p.u.)	-0.015	-0.005	1.039	2.5
Set point-3 (P_l = 118 kW, P_{PV} = 100 kW)				
Parameters	a_1	α	β	γ
Values (×10^{-6})	10000	100	0	200
Variables	P_B	Q_B	V_{611}	δ_{611}
Results (p.u.)	0.04	-0.005	1.052	4.5

to calculate the owed amount by a DNO for their network voltage correction.

V. Conclusion

Multiple stakeholders' involvement (e.g. customers and DNOs) is essential for use of novel resources in the smart grid that might have conflicting requirements. In this work, an optimization problem is formulated to find a trade-off between the BESS operation for voltage regulation. Network utilities are expected to operate with a 'customer-first' policy. Therefore, it is highly desirable to ensure that practical network support approaches are customer centric. The purpose of this paper is to propose and validate an approach that extracts network support benefits from customer BESS while simultaneously ensuring that cost to customers is minimized. The cost to customers is modeled as a convex disutility function. The disutility function used here is useful for modeling consumer preference and, therefore, the exact shape of the disutility function varies from customer to customer. Using the disutility function, a customer centric optimization problem is formulated for DN support through the appropriate charge/discharging of customer BESS units. The HIL real-time simulation results confirm that the proposed method can successfully control the BESS in a network for voltage regulation while reducing the overall cost. Parametric studies reveal that the approach presents sufficient flexibility to modify P_B, Q_B, voltage and δ for given load and PV conditions. An obstacle for the implementation of the proposed approach could be the computational burden, however, the HIL simulations show that the real-time operation is feasible.

References

[1] Y. Liu, J. Bebic, B. Kroposki, J. De Bedout, and W. Ren, "Distribution system voltage performance analysis for high-penetration PV," in *IEEE Energy 2030 Conference*. IEEE, 2008, pp. 1–8.

[2] "IEEE standard for interconnecting distributed resources with electric power systems," in *IEEE Std 1547-2003*. IEEE, 2003, pp. 1–28.

[3] N. Mahmud and A. Zahedi, "Review of control strategies for voltage regulation of the smart distribution network with high penetration of renewable distributed generation," *Renewable and Sustainable Energy Reviews*, vol. 64, pp. 582–595, 2016.

[4] K. E. Antoniadou-Plytaria, I. N. Kouveliotis-Lysikatos, P. S. Georgilakis, and N. D. Hatziargyriou, "Distributed and decentralized voltage control of smart distribution networks: models, methods, and future research," *IEEE Transactions on Smart Grid*, 2017.

[5] C. Long and L. F. Ochoa, "Voltage control of PV-rich LV networks: OLTC-fitted transformer and capacitor banks," *IEEE Transactions on Power Systems*, vol. 31, no. 5, pp. 4016–4025, 2016.

[6] E. Demirok, P. C. Gonzalez, K. H. Frederiksen, D. Sera, P. Rodriguez, and R. Teodorescu, "Local reactive power control methods for overvoltage prevention of distributed solar inverters in low-voltage grids," *IEEE Journal of Photovoltaics*, vol. 1, no. 2, pp. 174–182, 2011.

[7] X. Su, M. A. Masoum, and P. J. Wolfs, "Optimal PV inverter reactive power control and real power curtailment to improve performance of unbalanced four-wire LV distribution networks," *IEEE Transactions on Sustainable Energy*, vol. 5, no. 3, pp. 967–977, 2014.

[8] M. Kabir, Y. Mishra, G. Ledwich, Z. Y. Dong, and K. P. Wong, "Coordinated control of grid-connected photovoltaic reactive power and battery energy storage systems to improve the voltage profile of a residential distribution feeder," *IEEE Transactions on industrial Informatics*, vol. 10, no. 2, pp. 967–977, 2014.

[9] M. Rezkallah, A. Hamadi, A. Chandra, and B. Singh, "Real-time HIL implementation of sliding mode control for standalone system based on PV array without using dumpload," *IEEE Transactions On Sustainable Energy*, vol. 6, no. 4, pp. 1389–1398, 2015.

[10] M. Zeraati, M. E. H. Golshan, and J. Guerrero, "Distributed control of battery energy storage systems for voltage regulation in distribution networks with high PV penetration," *IEEE Transactions on Smart Grid*, vol. PP, no. 99, pp. 1–1, 2016.

[11] X. Liu, A. Aichhorn, L. Liu, and H. Li, "Coordinated control of distributed energy storage system with tap changer transformers for voltage rise mitigation under high photovoltaic penetration," *IEEE Transactions on Smart Grid*, vol. 3, no. 2, pp. 897–906, 2012.

[12] J. Tant, F. Geth, D. Six, P. Tant, and J. Driesen, "Multiobjective battery storage to improve PV integration in residential distribution grids," *IEEE Transactions on Sustainable Energy*, vol. 4, no. 1, pp. 182–191, 2013.

[13] N. Jayasekara, P. Wolfs, and M. A. Masoum, "An optimal management strategy for distributed storages in distribution networks with high penetrations of PV," *Electric Power Systems Research*, vol. 116, pp. 147–157, 2014.

[14] M. Bahramipanah, D. Torregrossa, R. Cherkaoui, and M. Paolone, "A decentralized adaptive model-based real-time control for active distribution networks using battery energy storage systems," *IEEE Transactions on Smart Grid*, vol. PP, no. 99, pp. 1–1, 2016.

[15] C. Zhao, U. Topcu, and S. H. Low, "Optimal load control via frequency measurement and neighborhood area communication," *IEEE Transactions on Power Systems*, vol. 28, no. 4, pp. 3576–3587, 2013.

[16] J. Brooks and P. Barooah, "Consumer-aware load control to provide contingency reserves using frequency measurements and inter-load communication," in *American Control Conference (ACC), 2016*. IEEE, 2016, pp. 5008–5013.

[17] "dSPACE 1103 PPC control board," https://www.dspace.com/en/inc/home/products/hw/singbord/ppcconbo.cfm, accessed: 24-04-2016.

[18] J. D. Glover, M. S. Sarma, and T. Overbye, *Power System Analysis & Design, SI Version*. Cengage Learning, 2012.

[19] G. Rothwell and T. Gomez, "Electricity economics," *IEEE series on power engineering*, 2003.

[20] S. Boyd and L. Vandenberghe, *Convex optimization*. Cambridge university press, 2004.

[21] "IEEE 13-bus feeder," https://ewh.ieee.org/soc/pes/dsacom/testfeeders/, accessed: 10-03-2015.

[22] C. Schauder and H. Mehta, "Vector analysis and control of advanced static VAR compensators," in *IEE Proceedings C (Generation, Transmission and Distribution)*, vol. 140, no. 4. IET, 1993, pp. 299–306.